

## **Brain imaging determinants of functional prognosis after severe endocarditis:**

### **A multicenter observational study.**

**Running head:** Predictors of Functional Prognosis in Endocarditis

Yves-Olivier GUETTARD, MD<sup>1§</sup>; Alexandre GROS, MD<sup>2§</sup>; Hikaru FUKUTOMI MD, PhD<sup>3</sup>;  
Xavier PILLOIS, PhD<sup>4</sup>; Sebastien PRÉAU, MD, PhD<sup>6</sup>; Yoan LAVIE-BADIE, MD<sup>7</sup>; Delphine  
MAREST, MD<sup>8</sup>; Raphaël P MARTINS, MD<sup>9</sup>; Elisabeth COUPEZ, MD<sup>10</sup>; Rémi COUDROY,  
MD, PhD<sup>11</sup>; Benjamin SEGUY, MD<sup>5</sup>; Alexandre BOYER, MD, PhD<sup>2\*</sup>; Thomas TOURDIAS,  
MD, PhD<sup>1,3\*</sup>; on behalf of the ICE-COCA investigators<sup>†</sup>

<sup>1</sup> Service de Neuroradiologie, CHU de Bordeaux, F-33000, France.

<sup>2</sup> Service de Médecine Intensive Réanimation, CHU de Bordeaux, F-33000, France.

<sup>3</sup> INSERM-U1215, Neurocentre Magendie, Bordeaux, F-33000, France.

<sup>4</sup> Hôpital Cardiologique du Haut-Lévêque, LIRYC Institute, Bordeaux, F-33000, France.

<sup>5</sup> Soins intensifs de cardiologie, Hôpital Cardiologique du Haut-Lévêque, CHU de Bordeaux, F-33000, France.

<sup>6</sup> Réanimation médicale, CHU de Lille, F-59000, France.

<sup>7</sup> Centre Expert de la valve, Fédération de Cardiologie, CHU de Toulouse, F-31000, France.

<sup>8</sup> Service d'Anesthésie-Réanimation, Hôpital Laënnec, CHU de Nantes, F-44000, France.

<sup>9</sup> Cardiologie et maladies vasculaires, CHU de Rennes, F-35000, France.

<sup>10</sup> Réanimation médicale polyvalente, CHU de Clermont-Ferrand, F-63000, France.

<sup>11</sup> Médecine Intensive Réanimation, CHU de Poitiers, F-86000, France and INSERM CIC 1402, groupe ALIVE, Université de Poitiers, F-86000, France.

#### **Corresponding author:**

Thomas Tourdias

Phone : +33 5 56 79 56 79

e-mail : thomas.tourdias@chu-bordeaux.fr

**Total number of tables and figures :** Tables 2 ; Figures 3

**Total word count:** 3511

**Abstract word count :** 250

<sup>§</sup> Both authors contributed equally to this work.

\* Pr. Boyer and Pr. Tourdias jointly directed this work and share co-senior authorship.

<sup>†</sup> A complete list of ICE-COCA investigators can be found in the Appendix at the end of the manuscript.

## **Brain imaging determinants of functional prognosis after severe endocarditis:**

### **A multicenter observational study.**

**Running head:** Predictors of Functional Prognosis in Endocarditis

#### **ABSTRACT**

**Objective:** We developed a detailed imaging phenotype of the cerebral complications in critically ill patients with infective endocarditis (IE) and determine whether any specific imaging pattern could impact prognostic information.

**Methods:** 192 patients admitted to the intensive care units of seven tertiary centers with severe, definite left IE and neurological complications were included. All underwent cerebral imaging few days after admission to define the types of lesions, their volumes, and their locations using voxel-based lesion-symptom mapping (VLSM). We employed uni- and multi-variate logistic regression analyses to explore the associations among imaging features and other prognostic variables and the 6-month modified Rankin Scale (mRS) score.

**Results:** Ischemic lesions were the most common lesions (75%; mean volume, 15.3±33 mL) followed by microbleeds (50%; mean number, 4±7.5), subarachnoidal hemorrhages (20%), hemorrhagic strokes (16%; mean volume, 14.6±21 mL), and hemorrhagic transformations (10%; mean volume, 5.6±11 mL). The volume of hemorrhagic transformations, the severity of leukopathy, and the compromises of certain locations on the motor pathway from the VLSM were associated with a poor 6-month mRS score on univariate analyses. However, upon multivariate analyses, no such specific imaging pattern independently predicted the mRS; this was instead influenced principally by age (OR=1.03 [1.004–1.06]) and cardiac surgery status (OR=0.06 [0.02–0.16]) in the entire cohort, and by age (OR=1.04 [1.01–1.08]) and *Staphylococcus aureus* status (OR=2.86 [1.19–6.89]) in operated patients.

**Conclusions:** In a cohort of severely ill IE patients with neurological complications, no specific imaging pattern could be highlighted as a reliable predictor of prognosis.

**KEYWORDS :** Infective endocarditis, stroke, topography, prognosis

## **BACKGROUND**

Infective endocarditis (IE) is associated with high-level mortality and severe complications [1]. Early prognosis (e.g., at admission) is crucial; the rapid identification of patients at highest risk prioritizes them for aggressive therapeutic approaches. For instance, heart failure and uncontrolled infection increase the risk of death [2]. Accordingly, these patients should be managed in a reference center with class I recommendation for emergency or urgent valve surgery according to the 2015 European Society of Cardiology guidelines [3].

The optimal management is much more debated for patients with neurological complications and especially critically ill patients admitted to intensive care unit (ICU) which is a particularly challenging sub-population. Cerebral complications have been associated with both early and late mortality [4-6]. However, neurological complications refer to a broad spectrum of complications that encompass most frequently ischemic strokes, but also cerebral hemorrhages, subarachnoidal hemorrhages (SAHs), intracranial infectious aneurysms (IIAs), and brain abscesses [7]. Outside the IE context, patient prognosis after ischemic or hemorrhagic stroke depends on both lesional volume [8, 9] and location [10] as revealed by cerebral imaging. Accumulating evidence also suggests that the health of the surrounding brain, thus “brain frailty,” significantly affects recovery from stroke [11, 12]. However, it remains unclear whether specific cerebral imaging patterns (e.g., lesional type, volume, location, and surrounding brain status) can predict the poor prognoses of critically ill IE patients. This is important; as no high-level management recommendation is available for those patients, some authors favor early surgery [13, 14], whereas others consider that valvular surgery should be postponed because this may cause further brain damage [15].

In this context, the objectives of this work from a multicenter observational cohort were (*i*) to provide a detailed picture of the spectrum of brain complications in severely ill patients with IE

using quantitative imaging, *(ii)* to seek specific brain imaging features associated with poorer functional outcomes overall and *(iii)* in patients who underwent valvular surgery.

## **METHODS**

### **Study Design and Patients**

Our present ICE-COCA (InfeCtious Endocarditis with Cerebral cOmplications: a Cohort from French reAnimations) study is a retrospective multicenter study that includes critically ill patients hospitalized with acute IEs in the surgical or medical ICUs of seven French tertiary-referral university hospitals (please see Appendix). All patients were consecutively screened from January 2010 to July 2017 and included if they met the following criteria: *(i)* definite, active (admission within 30 days of antibiotic commencement) left IE diagnosed using the modified Duke criteria [3]; *(ii)* neurological complications (symptomatic or not) documented by cerebral imaging prior to cardiac surgery; and, *(iii)* with severity criteria defined as Sequential Organ Failure Assessment (SOFA) score  $\geq 3$  justifying ICU admission. The exclusion criteria were isolated right endocarditis, in-hospital acquired endocarditis, and neurological complications that developed only after cardiac surgery. Retrospective database construction was approved by our local ethics committee (approval no. CE-SRLF-15-54) and the national data protection authority (declaration no. 2082557 v0) and complied with all dictates of the European Union General Data Protection Regulation in terms of protection of personal health data and personal information. Data were anonymized.

### **Data Collection at Inclusion**

We recorded age, gender, any history of endocarditis or valve surgery, and comorbidities (intravenous drug use, immunosuppression, diabetes mellitus, and renal insufficiency

[glomerular filtration rate <60 mL/min]). Care-associated IE was defined as early prosthetic valve IE (<12 months post-surgery) or nosocomial or non-nosocomial healthcare-associated IE [3]. Patient condition was assessed using SOFA and Glasgow Coma Scale (GCS) scores. Bacteria cultured from blood (n=174/192) and/or heart valves after surgery (n=35/101) were classified as *Staphylococcus aureus* or other bacteria, as in earlier prognostic studies [2]. Echocardiographic data included the involved valve, vegetation status and the maximum length thereof, and severe regurgitation status. In terms of therapy, the type of antibiotic was collected and the first day of treatment was chosen as day 0. Patients were all referred for cardiac surgery because of heart failure, uncontrolled infection, or a need to prevent an embolism, in line with the 2015 guidelines [3]. Despite at least one indication was present, the patient might not have been referred for surgery after multidisciplinary discussion because of severe comorbidities, multi-organ failure, or severe neurological complications. Surgical timing was recorded as “in line” or “delayed” by reference to the current recommendations [3] (emergency, urgent, or elective).

### **Neurological Complications**

All patients underwent brain imaging (before surgery, if surgery was performed) to assess neurological complications. Cerebral computed tomography (CT) or magnetic resonance imaging (MRI) was scheduled at the discretion of the investigating center, depending on availability and patient clinical status. When multiple scans were available, the scan performed closest to the time of surgery or the one that exhibited the largest lesional load was analyzed. When both CT and MRI scans were available, the MRI scans were preferred if the protocol included (at least) diffusion-weighted imaging (DWI), T2\*-weighted imaging (wi) fluid-attenuated inversion recovery (FLAIR), and 3D-T1 wi.-. Contrast-agent (iodine- or gadolinium-based) injection was not mandatory, but any in use was recorded. All scans were reviewed

centrally at the coordinating center (Bordeaux University Hospital) by a reader with 5 years of radiological experience blinded to both baseline and follow-up clinical data. For difficult cases, a senior neuroradiologist with 15 years of experience was consulted. We recorded ischemic lesions, intraparenchymal hemorrhages, SAHs, brain abscesses, and IIAs. Acute or subacute ischemic lesions were evident on CT scans as hypodense lesions and on DWI scans as hyperintense signals with restricted or normalized apparent diffusion coefficient (ADC). Intraparenchymal hemorrhages appeared as hyperdense lesions on CT scans and as hypointense signals on T2\*w scans and were classified as hemorrhagic transformations of ischemic strokes or primary hemorrhagic strokes depending on the imaging features. SAHs appeared as linear hyperdense regions on CT scans and hypointense areas that followed the shapes of the sulci on T2\*w scans. A cerebral abscess was defined as an expansive lesion exhibiting central ADC restriction, peripheral edema, and annular enhancement. An IIA was visualized as an additional vascular focal image evident on angiographic CT or MRI. Leukoaraiosis was evaluated considering that this is a major marker of small-vessel disease, the severity of which (brain frailty) is associated with functional outcomes after stroke [11, 12]. Leukoaraiosis was graded as low vs. high (equivalent to modified Fazekas score [16] 0 or 1 vs. score 2 or 3) to be comparable between CT and MRI [17]. Microbleeds (round hypointense regions <10 mm in diameter evident on T2\*wi [18]) were counted on MRI scans.

## **Image Analyses**

### **Lesional Segmentation**

Volume quantifications were performed at the coordinating center. Infarcts were segmented on CT or DWI scans, and intraparenchymal hemorrhage volumes were segmented on CT or T2\*w scans using the semiautomatic tools of 3D Slicer (<http://www.slicer.org>). Then, ischemic and

hemorrhagic lesional masks were registered to the MNI-152 template to compute prevalence maps (details in Supplemental Material).

### **Building maps of eloquent regions**

Lesional locations were quantified via voxel-based lesion-symptom mapping (VLSM), a method that has been widely validated to establish relationship between lesional presence or absence and a behavioral score on a voxel-by-voxel basis [19]. Only patients with ischemic and/or hemorrhagic lesions were analyzed in this manner. To enhance the statistical power, all lesions were flipped to the left hemisphere as previously described [10], and the ischemic and hemorrhagic maps were pooled to obtain global lesional maps. We then applied the VLSM method using the non-parametric mapping toolbox in the MRICron software package (ver. 15.6.2015) [20]. Repeatedly, for each individual voxel, patients were divided into two groups depending on whether the lesion affected the voxel, and modified Rankin Scale (mRS) scores at 6 months were compared between the groups with and without lesions using the Brunner-Munzel rank order test. Only voxels affected in  $\geq 10$  subjects were tested, to avoid artificial inflation of the Brunner-Munzel scores. Such important threshold is the main reason why we had to pool ischemic and hemorrhagic events together and to flip them so that we could increase the probability of having as many voxels as possible affected at least 10 times in our population. The small and randomly distributed lesions of infective endocarditis prevented the possibility to run hemispheric-specific analysis. The resulting Z-score maps were controlled for multiple comparisons via false-discovery rate correction, to ensure a false-positive  $P$ -value  $< 0.05$ . Thus, VLSM-mapped lesioned voxels that were significantly associated with the 6-month functional outcomes. Informative regions were identified using the Harvard-Oxford cortical and subcortical structural atlases of the Harvard Center for Morphometric Analysis and the JHU DTI-based white-matter atlases of the Laboratory of Brain Anatomical MRI (Johns Hopkins



University) [21] incorporated in the FSL software package. Next, to include location in a multivariate context (thus, with other contributors to functional outcomes), we computed a metric that we termed an “eloquent area” using a validated method [22]; this is described below. Briefly, an eloquent-area mask was created using the VLSM map based on significant Z-scores reflecting 5% false-discovery thresholds. Next, the lesional volume within each eloquent area was calculated by overlaying individual lesional binary masks on the eloquent-area masks.

### **Follow-up**

At the 6-month follow-up, the extent of neurological handicap was evaluated by using the mRS score either face-to-face or via a telephone interview as validated [23]; all interviewers were blinded to the initial imaging data.

### **Statistical Analyses**

Continuous variables are expressed as the means  $\pm$  standard deviations. Categorical variables are expressed as the numbers of observations with percentages (%). The Shapiro-Wilk test was used to assess normality. The dependent variable was the functional outcome at 6 months as assessed by the mRS score dichotomized (using a clinically relevant threshold) as good when mRS score < 3 (ability to walk without assistance) and poor otherwise (mRS score  $\geq$  3)[24]. Independent variables were first compared between the good- and poor-outcome groups with descriptive statistics. Continuous variables were compared using an independent-samples parametric test (the unpaired Student t-test) or a non-parametric test (the Mann-Whitney test), as appropriate. Categorical variables were compared using the Fisher exact test or  $\chi^2$  test, as appropriate. Then, the associations were subjected to uni- and multivariate logistic regression via backward stepwise analyses in which variables associated with *P*-values < 0.2 from the univariate analyses were included. All analyses were also performed independently for patients

who were operated upon. All tests were two-sided and a  $P$ -value  $<0.05$  was considered to indicate statistical significance. All analyses were performed with the aid of IBM SPSS Statistics ver. 17.0 software.

## RESULTS

### Study Population

Patient characteristics are summarized in Table 1. The mean age was 60 years, and 69% of the patients (133/192) were male. In terms of comorbidities, 26% (50/192) had a history of valve surgery, 27% (51/192) had diabetes, and 40% (76/192) exhibited renal insufficiency. IE was care-associated in 23%, and 54% had *S. aureus* infections (104/192). Echocardiography revealed vegetations in 91% (174/192) of the patients, with a mean length of 16 mm ( $\pm$  10.2 mm) and severe regurgitation in 60% (115/192). Such patients were severely ill, with a mean SOFA score of 7.7 ( $\pm$  4), a mean GCS score of 11.7 ( $\pm$  4), and compromised consciousness in 132 patients (69%). All such patients were indicated for early surgery; 65% (125/192) did in fact undergo surgery; the others were denied surgery by our multidisciplinary team. **Supplemental Table I** summarizes the surgical indications and timings. At the 6-month follow-up, the functional outcomes were good (mRS score <3) in 43.7% (84/192) of the patients and poor (mRS score  $\geq$ 3) in 56.2% (108/192); the latter group included 39.6% of patients (76/192) who died (mRS score =6).

### Cerebral Imaging

Brain MRI was performed on 47% (90/192) of the patients and CT on 53% (102/192). A contrast agent was injected during most explorations (83%, 160/192). Ischemic lesions were the most frequent findings found in 75% of the patients (143/192), more frequently in those evaluated via MRI compared to CT, as shown by the mean frequency maps (**Figure 1a–c**). In patients with ischemic lesions, the mean volume was 15.3 mL ( $\pm$  33 mL). Typically, patients had scattered small lesions with or without larger territorial strokes (**Figure 2a–b**). All the territories could be involved with a higher frequency for the middle cerebral artery territory (**Figure 1c**). Brain hemorrhage reflected hemorrhagic stroke in 16% of the patients (30/192;

mean volume  $14.6 \pm 21$  mL) and hemorrhagic transformation of an ischemic lesion in 10% (20/192; mean volume  $5.6 \pm 11$  mL). The proportions of hemorrhagic lesions were identical in patients evaluated via MRI and CT (**Figure 1d–f**); the lesions occurred randomly within the brain. The microbleed prevalence was high; at least one microbleed was found in 50% of the patients who underwent MRI (45/90), and the mean microbleed number was  $4 (\pm 7.5)$ . The microbleeds were both peripheral and deep (**Figure 2c**). SAHs were found in 20% of the patients (38/192), but other complications were rarer—IAs were found in 9% of the patients (18/192) and brain abscesses in only three patients. IAs were frequently accompanied by intracranial hemorrhages (**Figure 2d**).

### **Results of VLSM Analysis**

Of the 192 patients, 144 were subjected to VLSM analysis while 48 had to be excluded from such analysis either because they had no ischemic or hemorrhagic lesions ( $n=8$ ) or because of failure of registration to the MNI space ( $n=40$ ). The VLSM maps in **Figure 3** (featuring color-coded overlays) show that specific lesion locations (ischemic or hemorrhagic) were significantly associated with the mRS score at 6 months. Especially, VLSM revealed that the motor pathway brain regions (the pre-central region and corona radiata) significantly influenced the scores (details in **Table 2**).

### **Factors Associated with 6-month Functional Outcomes**

When the initial imaging metrics were compared to the mRS scores at 6 months (**Table 1**), we confirmed that higher lesional volumes in eloquent areas were associated with poor functional outcomes (3.1 vs. 1.1 mL,  $P=0.01$ ). Also, higher-volume of hemorrhagic transformation (8 vs. 2.6 mL,  $P<0.001$ ) and a tendency toward more leukopathy ( $P=0.061$ ) were associated with poor functional outcomes. However, neither ischemic stroke (presence or volume) nor primary

hemorrhage (presence or volume) were associated with functional outcomes. Surprisingly, IIAs were less frequent in the poor-outcome group (4% vs. 17%,  $P=0.002$ ). Contrast agents were less frequently injected into patients in the poor-outcome group (79% vs. 89%,  $p=0.051$ ); perhaps complicating the above observation as contrast is essential to detect IIA.

The other factors associated with poor functional outcomes were frailty (older age, previous valve surgery, diabetes, and renal insufficiency), the initial clinical severity (higher SOFA score and lower GCS score), and a failure to be scheduled for cardiac surgery because of prohibitive risk. Severe regurgitation was more frequent in the good-outcome group (77% vs. 60%,  $P=0.02$ ).

After multivariate analysis, the only two factors that remained independently associated with a poor functional outcome were older age (odds ratio [OR]=1.03 [1.004–1.06],  $P=0.023$ ) and no surgery (OR=0.06 [0.02–0.16],  $P<0.001$ ).

As surgery was deemed a strong predictor of functional outcome in this cohort of critically ill patients, we performed two sensitivity analyses. We first ran the same multivariate model on the total population ( $n=192$ ) without surgery within the independent variables. It showed that the factors independently associated with poor outcomes were still older age (OR=1.03 [1.01–1.06],  $P=0.05$ ) together with a higher initial SOFA score (OR=1.18 [1.07–1.29],  $P=0.001$ ), and a higher volume compromise in eloquent areas (OR=1.09 [1.01–1.18],  $P=0.035$ ). We also repeated this analysis on patients who underwent surgery ( $n=125$ ) to detect brain imaging predictors in such patients (**Supplemental Table II**). Leukopathy was the only brain feature associated with a poor outcome upon univariate analysis (63% vs. 42%,  $P=0.023$ ), but the significance disappeared upon multivariate analysis; poor prognosis was independently associated with only older age (OR=1.04 [1.01–1.08],  $P=0.015$ ) and *S. aureus* infection status (OR=2.86 [1.19–6.89],  $P=0.02$ ).

## DISCUSSION

Cerebral imaging detects frequent ischemic and hemorrhagic lesions during complicated IE whose phenotype, including lesion subtype, volume and location, can be precisely assessed. However, in severely ill patients, the functional outcomes at 6 months were not independently predicted by any specific imaging feature, but only by age, failure to undertake cardiac surgery when indicated and *S. aureus* infection status.

Neurological complications are frequently encountered in IE patients. Multicenter registries that include patients with a wide panel of severities report neurological complications in 20–25% [6], while frequency reached 55% in a cohort of patients admitted to ICUs [5]. It is important to note that brain imaging was not systematic in these previous studies; embolic events can even be detected more frequently when systematic cerebral MRI is performed [25]. In that sense, our cohort data are particularly valuable because all patients underwent brain imaging. We confirmed here the strong prevalence of ischemic events that concerned 75% of the patients and we also highlighted the frequency of hemorrhagic lesions such as microbleeds, SAHs, and hemorrhagic stroke and their coexistence besides ischemic lesions in severely ill IE patients. This proportion might have been impacted by the fact that approximately half of our patients underwent MRI, which detects ischemia more sensitively than does CT [26]. In line with this statement, our frequency maps showed more ischemic lesions when MRI was used which is not the case for hemorrhagic lesions where CT and T2\* are known to have close performances [27]. Having neurological complication was one of the inclusion criteria and therefore the high prevalence of *Staphylococcus Aureus* and severe valvular damages of our population was expected as these factors have been associated with neurological events in previous studies [2, 7, 28].

Importantly, the neurological complications of IE are very heterogeneous in nature and imaging severity, but the IE literature does not adequately reflect this. Here, our univariate analyses

showed that functional outcomes were worse when hemorrhage developed compared to patients experiencing ischemic events only, in line with previous literature [14]. One might speculate that small lesions affect functional outcomes to a lesser extent than do larger strokes, but we found that ischemic volume was not significantly associated with functional outcome. In patients suffering strokes outside the context of IE, ischemic volume is only moderately correlated with functional outcome; [29] indicating that other factors are in play. Our observed lack of a correlation in IE patients was thus not entirely unexpected in IE in which stroke heterogeneity is bigger than in strokes unrelated to IE. As lesions in eloquent areas may have strong functional impacts, it is important to consider lesional location when trying to predict outcomes in various functional domains [10, 22]. In our analysis, that is the first to consider lesional patterns of lesions on a voxel-by-voxel in IE, maps highlighted specific locations along the motor pathway but also surrounding the insula and the opercular cortex as particularly relevant, which is in lines with stroke data [10, 30]. The metric termed “volume of eloquent area” was significantly associated with functional outcome. It is also interesting to note that the severity of leukopathy, a major marker of small-vessel disease, was associated with poorer outcomes in patients who underwent operations. This adds to the emerging concept that outcomes are determined not only by the nature of the stroke but also by the health of the surrounding brain [11, 12].

Despite the associations evident in univariate analyses, such detailed patterns of brain damages did not persist as independent predictors of outcomes; rather, these were age, cardiac surgery status, and *S. aureus* infection status. Neurological complications (regardless of pattern) have been associated with elevated mortality and greater numbers of sequelae in previous papers [3-6]. Here, we recruited a cohort of severely ill patients with neurological complications in all of them and our data indicate that, in those particularly severe patients who required ICU

hospitalization, more imaging precisions on the types, volumes or locations the cerebral lesions are not strong enough to convey additional prognosis information.

The strengths of our study include its multicentric nature and the fact that we enrolled one of the largest populations to date of patients with severe IE, who pose very challenging management issues. This is also one of the rare studies in which all the patients have been explored with brain imaging centrally reviewed with application of quantitative metrics to provide a detail phenotype of the neurological complications. However, our work had certain limitations. Selection and referral biases might have been in play, as this was a retrospective cohort originating from tertiary centers. Imaging protocols differed among the centers, creating heterogeneity such as for IIA detection in relation with inconstant use of contrast agent. Similarly, it is likely that extend of brain lesions might have been under-estimated in patients explored only with CT, but the type of examination (CT or MRI) was well balanced in the poor vs. good outcome groups. We also have to acknowledge that eloquence of location could not consider any possible right-left asymmetry because we had not enough voxels similarly affected in enough patients without flipping all the lesions to the left hemisphere. Importantly, patients such as those of this study face major decision-making problems, as both indications and contra-indications for cardiac surgery co-existed [3]. Some authors suggest early surgery even for cases with brain hemorrhages, whereas others suggest delay [14, 15]. A decision to proceed with surgery by the endocarditis team is therefore certainly influenced by the imaging pattern [31] and such interaction might not be fully compensated for by the multivariate analyses. Similarly, the fewer imaged lesions in the surgery subgroup might have made it difficult to define the predictive value of an imaging pattern, because not all patterns were well-represented. Only randomized trial would allow concluding formally on the impact of imaging patterns unbiased from surgery but this is ethically difficult to conduct. It is also possible that



mortality unrelated to neurological complications might have decreased the strength of any association between a cerebral imaging pattern and the mRS score.

Despite these limitations, our data support the fact that, in severely ill IE patients with neurological complications managed by reference to the current guidelines[3], no quantitative imaging pattern is more poorly prognostic than any other. Whether those severe patients should be referred for surgery regardless of imaging pattern is the following question that will require further investigations.

## **CONCLUSIONS**

In a cohort of severely ill IE patients with neurological complications, no specific imaging pattern could be highlighted as a reliable predictor of prognosis.

## **LIST OF ABBREVIATIONS**

ADC: Apparent Diffusion Coefficient

DWI: Diffusion-weighted Imaging

ESC: European Society of Cardiology

FLAIR: Fluid-attenuated Inversion Recovery

ICE-COCA: InfeCtious Endocarditis with Cerebral cOmplications: a Cohort from French reAnimations

ICU: Intensive Care Unit

IE: Infective Endocarditis

IIA: Infectious Intracranial Aneurysm

mRS: modified Rankin Scale

SAH: Subarachnoidal Hemorrhage

SOFA: Sequential Organ Failure Assessment

VLSM: Voxel-based Lesion Symptom Mapping

## REFERENCES

1. Cahill, T.J. and B.D. Prendergast, *Infective endocarditis*. *Lancet*, 2016. **387**(10021): p. 882-93.
2. Murdoch, D.R., et al., *Clinical presentation, etiology, and outcome of infective endocarditis in the 21st century: the International Collaboration on Endocarditis-Prospective Cohort Study*. *Arch Intern Med*, 2009. **169**(5): p. 463-73.
3. Habib, G., et al., *2015 ESC Guidelines for the management of infective endocarditis: The Task Force for the Management of Infective Endocarditis of the European Society of Cardiology (ESC). Endorsed by: European Association for Cardio-Thoracic Surgery (EACTS), the European Association of Nuclear Medicine (EANM)*. *Eur Heart J*, 2015. **36**(44): p. 3075-3128.
4. Garcia-Cabrera, E., et al., *Neurological complications of infective endocarditis: risk factors, outcome, and impact of cardiac surgery: a multicenter observational study*. *Circulation*, 2013. **127**(23): p. 2272-84.
5. Sonnevile, R., et al., *Neurologic complications and outcomes of infective endocarditis in critically ill patients: the ENDOcardite en REAnimation prospective multicenter study*. *Crit Care Med*, 2011. **39**(6): p. 1474-81.
6. Habib, G., et al., *Clinical presentation, aetiology and outcome of infective endocarditis. Results of the ESC-EORP EURO-ENDO (European infective endocarditis) registry: a prospective cohort study*. *Eur Heart J*, 2019. **40**(39): p. 3222-3232.
7. Lung, B., et al., *Determinants of cerebral lesions in endocarditis on systematic cerebral magnetic resonance imaging: a prospective study*. *Stroke*, 2013. **44**(11): p. 3056-62.
8. Vogt, G., et al., *Initial lesion volume is an independent predictor of clinical stroke outcome at day 90: an analysis of the Virtual International Stroke Trials Archive (VISTA) database*. *Stroke*, 2012. **43**(5): p. 1266-72.
9. Broderick, J.P., et al., *Volume of intracerebral hemorrhage. A powerful and easy-to-use predictor of 30-day mortality*. *Stroke*, 1993. **24**(7): p. 987-93.
10. Wu, O., et al., *Role of Acute Lesion Topography in Initial Ischemic Stroke Severity and Long-Term Functional Outcomes*. *Stroke*, 2015.
11. Appleton, J.P., et al., *Imaging markers of small vessel disease and brain frailty, and outcomes in acute stroke*. *Neurology*, 2020. **94**(5): p. e439-e452.

12. Ryu, W.S., et al., *Stroke outcomes are worse with larger leukoaraiosis volumes*. *Brain*, 2017. **140**(1): p. 158-170.
13. Kang, D.H., et al., *Early surgery versus conventional treatment for infective endocarditis*. *N Engl J Med*, 2012. **366**(26): p. 2466-73.
14. Wilbring, M., et al., *The impact of preoperative neurological events in patients suffering from native infective valve endocarditis*. *Interact Cardiovasc Thorac Surg*, 2014. **18**(6): p. 740-7.
15. Yoshioka, D., et al., *Impact of early surgical treatment on postoperative neurologic outcome for active infective endocarditis complicated by cerebral infarction*. *Ann Thorac Surg*, 2012. **94**(2): p. 489-95; discussion 496.
16. Fazekas, F., et al., *MR signal abnormalities at 1.5 T in Alzheimer's dementia and normal aging*. *AJR Am J Roentgenol*, 1987. **149**(2): p. 351-6.
17. Rudilosso, S., et al., *Evaluation of white matter hypodensities on computed tomography in stroke patients using the Fazekas score*. *Clin Imaging*, 2017. **46**: p. 24-27.
18. Greenberg, S.M., et al., *Cerebral microbleeds: a guide to detection and interpretation*. *Lancet Neurol*, 2009. **8**(2): p. 165-74.
19. Bates, E., et al., *Voxel-based lesion-symptom mapping*. *Nat Neurosci*, 2003. **6**(5): p. 448-50.
20. Rorden, C., H.O. Karnath, and L. Bonilha, *Improving lesion-symptom mapping*. *J Cogn Neurosci*, 2007. **19**(7): p. 1081-8.
21. Tzourio-Mazoyer, N., et al., *Automated anatomical labeling of activations in SPM using a macroscopic anatomical parcellation of the MNI MRI single-subject brain*. *Neuroimage*, 2002. **15**(1): p. 273-89.
22. Munsch, F., et al., *Stroke Location Is an Independent Predictor of Cognitive Outcome*. *Stroke*, 2016. **47**(1): p. 66-73.
23. Janssen, P.M., et al., *Comparison of telephone and face-to-face assessment of the modified Rankin Scale*. *Cerebrovasc Dis*, 2010. **29**(2): p. 137-9.
24. Broderick, J.P., O. Adeoye, and J. Elm, *Evolution of the Modified Rankin Scale and Its Use in Future Stroke Trials*. *Stroke*, 2017. **48**(7): p. 2007-2012.
25. Hess, A., et al., *Brain MRI findings in neurologically asymptomatic patients with infective endocarditis*. *AJNR Am J Neuroradiol*, 2013. **34**(8): p. 1579-84.
26. Goulenok, T., et al., *Infective endocarditis with symptomatic cerebral complications: contribution of cerebral magnetic resonance imaging*. *Cerebrovasc Dis*, 2013. **35**(4): p. 327-36.

27. Kidwell, C.S., et al., *Comparison of MRI and CT for detection of acute intracerebral hemorrhage*. JAMA, 2004. **292**(15): p. 1823-30.
28. Di Salvo, G., et al., *Echocardiography predicts embolic events in infective endocarditis*. J Am Coll Cardiol, 2001. **37**(4): p. 1069-76.
29. Johnston, K.C., et al., *Validation of an acute ischemic stroke model: does diffusion-weighted imaging lesion volume offer a clinically significant improvement in prediction of outcome?* Stroke, 2007. **38**(6): p. 1820-5.
30. Cheng, B., et al., *Influence of stroke infarct location on functional outcome measured by the modified rankin scale*. Stroke, 2014. **45**(6): p. 1695-702.
31. Duval, X., et al., *Effect of early cerebral magnetic resonance imaging on clinical decisions in infective endocarditis: a prospective study*. Ann Intern Med, 2010. **152**(8): p. 497-504, W175.

## **SUPPLEMENTARY INFORMATION**

Expanded materials and methods

Supplemental tables I and II

## **DECLARATIONS**

### **1- Funding**

None.

### **2- Competing interests**

On behalf of all authors, the corresponding author states that there is no conflict of interest

### **3- Availability of data and materials**

The datasets used during the current study are available from the corresponding author on reasonable request.

### **4- Code availability**

Not applicable

### **5- Authors' contributions**

TT and AB designed the study. YOG, AG and HF collected the data. YOG, HF and TT wrote the manuscript. All authors read and approved the final manuscript.

### **6- Ethics approval and consent to participate**

Retrospective database construction was approved by our local ethics committee (approval no. CE-SRLF-15-54) and the national data protection authority (declaration no. 2082557 v0) and complied with all dictates of the European Union General Data Protection Regulation in terms of protection of personal health data and personal information.

### **7- Consent for publication**

Not applicable.

## **APPENDIX**

### **The ICE-COCA research investigators:**

Bordeaux University Hospital : Pr BOYER Alexandre, Pr GRUSON Didier and Dr GROS Alexandre, Service de Médecine Intensive Réanimation, Pr COSTE Pierre and Dr SEGUY Benjamin, Soins intensifs de cardiologie, Hôpital Cardiologique du Haut-Lévêque, Pr TOURDIAS Thomas and Dr GUETTARD Yves-Olivier, Service de Neuroradiologie.

Clermont-Ferrand University Hospital: Dr SOUWEINE Bertrand and Dr COUPEZ Elisabeth, Médecine intensive et réanimation.

Lille University Hospital: Pr PREAU Sébastien, Pr NSEIR Saad and Dr TOUSSAINT Aurélia, Réanimation médicale, Dr OUTTERYCK Olivier, service de neuroradiologie.

Nantes University Hospital: Pr REIGNIER Jean and Dr MAREST Delphine, Service d'Anesthésie-Réanimation.

Poitiers University Hospital: Pr ROBERT René and Dr COUDROY Rémi, Médecine Intensive Réanimation.

Rennes University Hospital: Dr MARTINS Raphaël, Cardiologie et maladies vasculaires, and Dr URIEN Jean Marie, service de cardiologie, groupe hospitalier Bretagne sud.

Toulouse University Hospital: Dr PORTE Lydie, Département de maladies infectieuses; Dr LAVIE-BADIE Yoan, Dr ROBIN Guillaume and Dr CHARBONNIER Gaëtan, Centre expert de la valve, fédération de cardiologie; Dr SARTON Benjamine and Pr SILVA Stein, Réanimation polyvalente adultes.

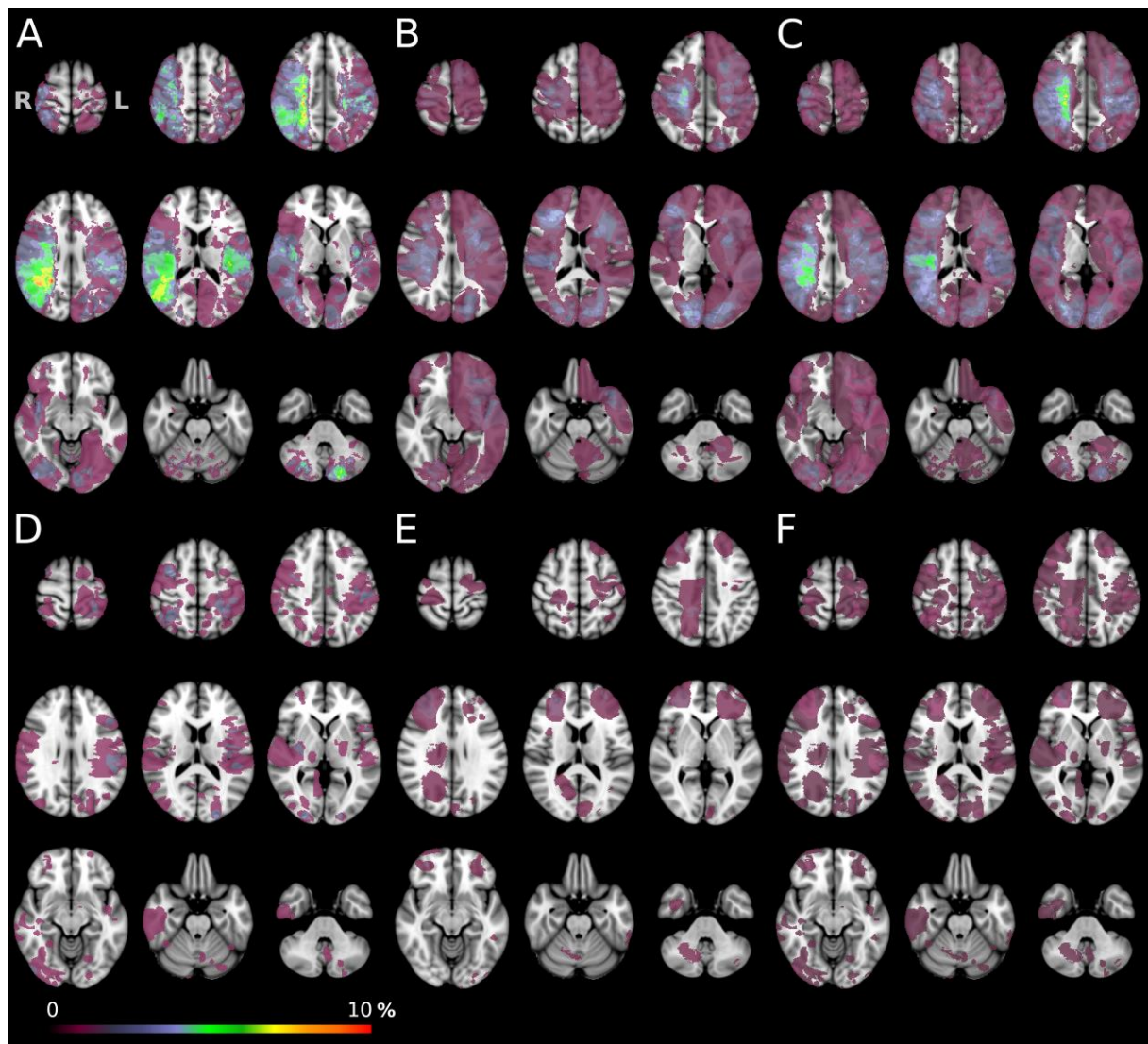
**FIGURES****Figure 1**



Figure 2

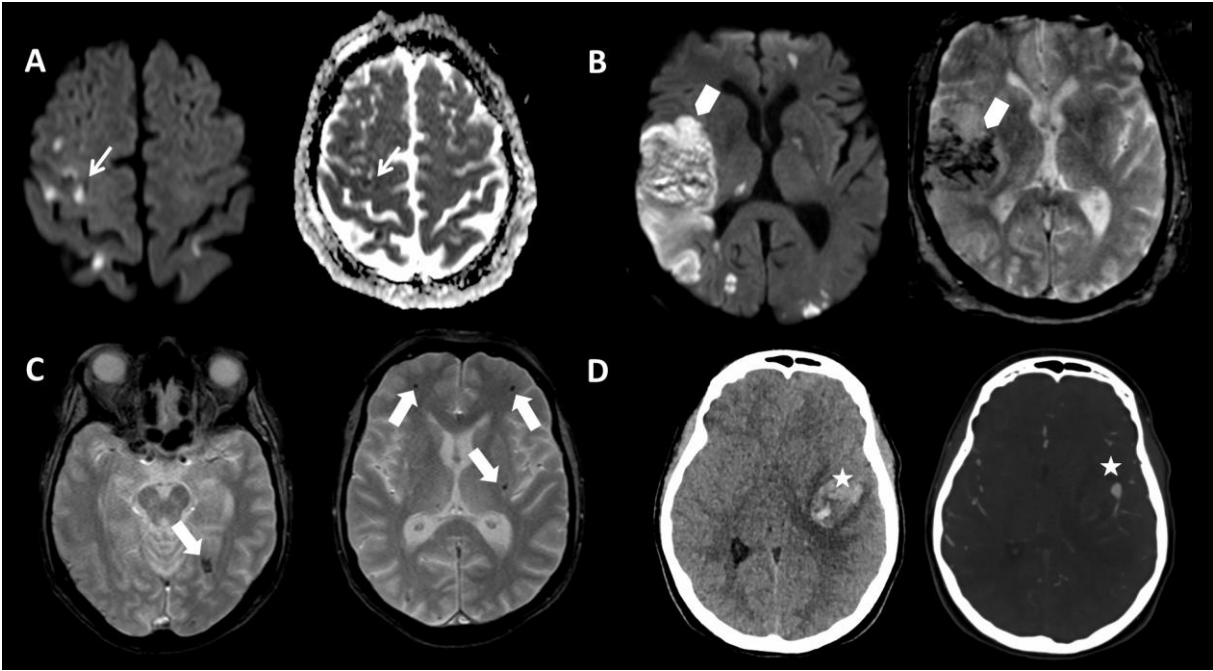
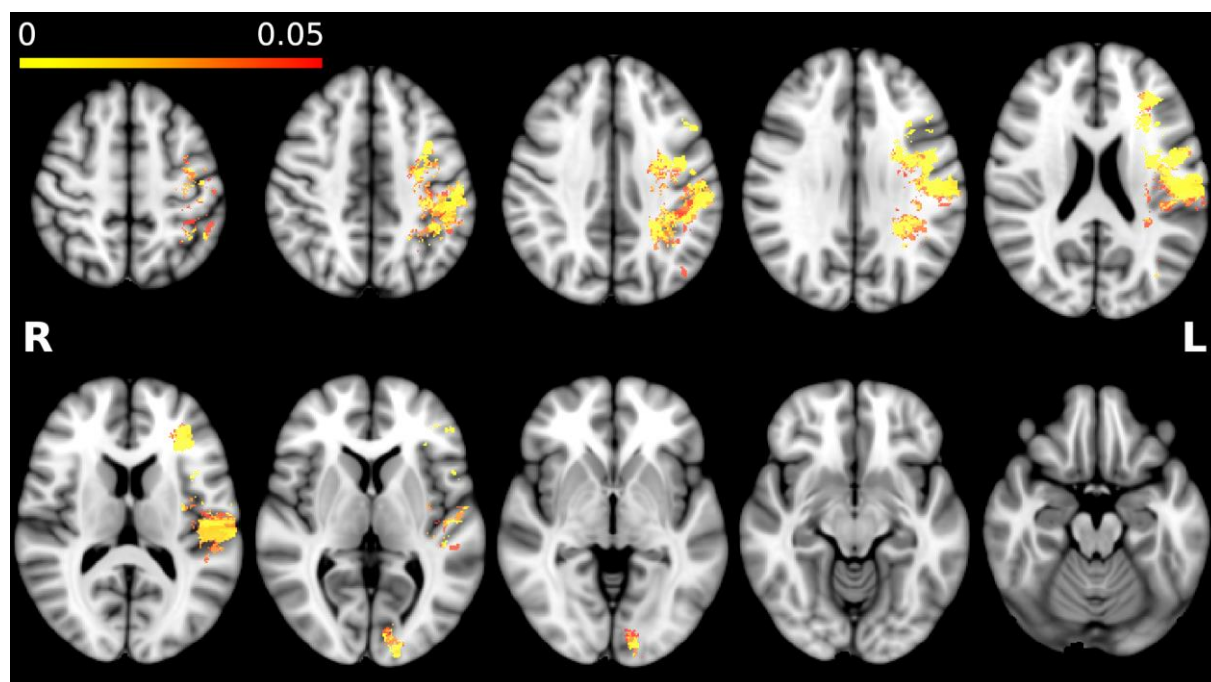


Figure 3



## FIGURE LEGENDS

**Figure 1:** Frequency maps of ischemic lesions based on diffusion-weighted imaging (DWI) (A), computed tomography (CT) (B), and pooled DWI and CT (C). Frequency maps of hemorrhagic lesions based on T2\*-weighted images (D), CT (E), and pooled T2\*-weighted images and CT (F). The color bar indicates the frequency of overlapping lesions. R, right; L, left.

**Figure 2:** Examples of cerebral lesions. (A) multiple small ischemic lesions evident on DWI with restricted apparent diffusion coefficient (thin arrows), (B) territorial infarcts evident on DWI with hemorrhagic transformations apparent in T2\*-weighted images (arrowheads), (C) multiple microbleeds apparent in T2\*-weighted images (thick arrows), and (D) intraparenchymal hemorrhages secondary to infectious intracranial aneurysms evident on CT (stars).

**Figure 3:** Voxel-based lesion-symptom mapping of the impact on modified Rankin Scale (mRS) score at 6 months, overlaid on T1 MNI-152 atlas. All lesions (ischemic and hemorrhagic) were flipped to the left hemisphere. The colors denote the *P*-values of Brunner-Menzel tests. R, right; L, left.

## **TABLES**

**Table 1. Variables associated with functional outcomes based on the mRS score at 6 months (univariate analyses).**

	Total population (n=192)	mRS <3 (n=84)	mRS ≥3 (n=108)	P-value
Patient characteristics				
Age (years)*	60 (± 14)	56 (± 15)	63 (± 13)	<b>0.003</b>
Sex, male	133 (69)	54 (64)	79 (73)	0.187
Prior endocarditis	11 (6)	3 (4)	8 (8)	0.253
Prior valve surgery	50 (26)	15 (18)	35 (32)	<b>0.023</b>
Intravenous drug use	19 (10)	11 (14)	8 (8)	0.198
Immunosuppression	21 (11)	7 (8)	14 (13)	0.308
Diabetes mellitus	51 (27)	16 (19)	35 (32)	<b>0.038</b>
Renal insufficiency	76 (40)	26 (31)	50 (46)	<b>0.031</b>
Care-associated condition	45 (23)	14 (17)	31 (29)	0.051
Clinical and microbiological features				
SOFA score*	7.7 (± 4)	6.6 (± 3.6)	8.5 (± 4.2)	<b>0.001</b>
Glasgow Coma Scale score*	11.7 (± 4)	12.6 (± 3)	10.9 (± 4)	<b>0.002</b>
<i>Staphylococcus aureus</i> infection	104 (54)	41 (49)	63 (58)	0.189
Echocardiographic findings				
Aortic valve involved	125 (65)	53 (63)	72 (67)	0.607
Mitral valve involved	106 (55)	46 (55)	60 (56)	0.913
Aortic and mitral valves involved	66 (34)	31 (37)	35 (33)	0.625
Vegetation	174 (91)	79 (94)	95 (88)	0.151
Vegetation length (mm)*	16 (± 10.2)	16 (± 12)	16 (± 9)	0.977
Regurgitation ≥3/4	115 (60)	58 (77)	57 (62)	<b>0.026</b>
Therapy				
Cardiac surgery	125 (65)	77 (92)	48 (44)	<b>&lt;0.001</b>
Brain imaging findings				
MRI	90 (47)	42 (50)	48 (44)	0.444
Contrast injection	160 (83)	75 (89)	85 (79)	0.051
Time from diagnosis (days)*	6 (± 21)	6 (± 17)	6 (± 24)	0.795
Ischemic stroke	143 (75)	60 (71)	83 (77)	0.393
Ischemic volume (mL)*	15.3 (± 33)	11 (± 19)	19 (± 40)	0.144
Hemorrhagic transformation	20 (10)	9 (11)	11 (10)	0.905
Hemorrhagic transformation volume (mL)*	5.6 (± 11)	2.6 (± 2.2)	8 (± 15)	<b>&lt;0.001</b>
Hemorrhagic stroke	30 (16)	14 (17)	16 (15)	0.726
Hemorrhagic stroke volume (mL)*	14.6 (± 21)	14.1 (± 20)	15.1 (± 23)	0.891
Total hemorrhagic volume (mL)*	11 (± 18)	9.6 (± 16)	12.2 (± 20)	0.611
Subarachnoidal hemorrhage	38 (20)	18 (21)	20 (19)	0.616
Abscess	3 (2)	2 (2)	1 (1)	0.420
IIA	18 (9)	14 (17)	4 (4)	<b>0.002</b>
Leukopathy	97 (51)	36 (43)	61 (57)	0.061
Microbleeds (n)*	4 (7.5)	5.2 (9.4)	2.9 (5.2)	0.167
Volume of the eloquent area	2.9 (±7)	1.1 (±3)	3.1 (±7)	<b>0.011</b>

Notes: Unless otherwise specified, the data are numbers of participants with percentages in parentheses. For each category, data were missing for fewer than five participants (e.g., intravenous drug users) and thus available for at least 184 participants. Brain abscess data were available for 160 participants who received injections, and eloquent area volumes for 144 participants with ischemic or hemorrhagic lesions exhibiting good-quality co-registrations with the MNI space.

\* Means  $\pm$  standard deviations.

Mean microbleed volumes and numbers were calculated using data from patients affected by such events.

SOFA, Sequential Organ Failure Assessment; MRI, magnetic resonance imaging; IIA, infectious intracranial aneurysm.

**Table 2. The principal eloquent functional regions as revealed by voxel-based lesion-symptom mapping.**

Principal eloquent regions	Mean Z-score $\pm$ SD
Middle frontal gyrus	2.60 $\pm$ 0.37
Inferior frontal gyrus, pars opercularis	2.52 $\pm$ 0.09
Anterior corona radiata	2.37 $\pm$ 0.34
Postcentral gyrus	2.27 $\pm$ 0.37
Central opercular cortex	2.26 $\pm$ 0.31
Inferior frontal gyrus, pars triangularis	2.25 $\pm$ 0.14
Precentral gyrus	2.23 $\pm$ 0.31
Left cerebral white matter	2.20 $\pm$ 0.39
Superior longitudinal fasciculus	2.16 $\pm$ 0.38
Posterior corona radiata	2.15 $\pm$ 0.39

Data are presented as the means and standard deviations (SDs) of the z-scores of the template regions listed in the Harvard-Oxford Cortical Structural Atlas and the JHU ICBM-DTI-81 White Matter Labels. The regions are listed by their highest mean z-values, in descending order.